ACS OMEGA

Open Access

http://pubs.acs.org/journal/acsodf

Article

Synthesis, Properties, and Techno-economic Analysis of Highly Stable Biotransformer Oil Derived from Transesterification of Palm Oil Methyl Esters and Ditrimethylolpropane

Ratchayol Sornvoralop, Benjapon Chalermsinsuwan, Nathapol Pintuyothin, Boonyawan Yoosuk,* and Napida Hinchiranan*

Cite This: *ACS Omega* 2024, 9, 42396−42409

Read Online

ACCESS | Metrics & More | Article Recommendations | Supporting Information

ABSTRACT: Currently, biotransformer oil (BTO) is in high demand due to the increasing level of electrical power consumption and environmental policy. Hence, this research aimed to prepare a highly stable BTO via basic transesterification of palm oil methyl ester (POME) and ditrimethylolpropane (Di-TMP) catalyzed by sodium methoxide ($NaOCH_3$). Under the optimal conditions (POME/Di-TMP molar ratio = 5.0/1.0, $NaOCH_3$ loading = 8 mol % based on the Di-TMP content under 3.5 mbar, and 300 rpm at 160 °C for 2 h), the POME conversion level and POME-Di-TMPTTE selectivity reached 90.3% and 96.6%, respectively. The obtained BTO with a high POME-Di-TMPTTE portion exhibited greater oxidation stability with a higher flash point and breakdown voltage in accordance with the IEC 62770 specification. A techno-economic analysis revealed the possibility of POME-Di-TMPTTE as a commercial BTO for its competitive cost and profit based on the current commercial price of BTO.

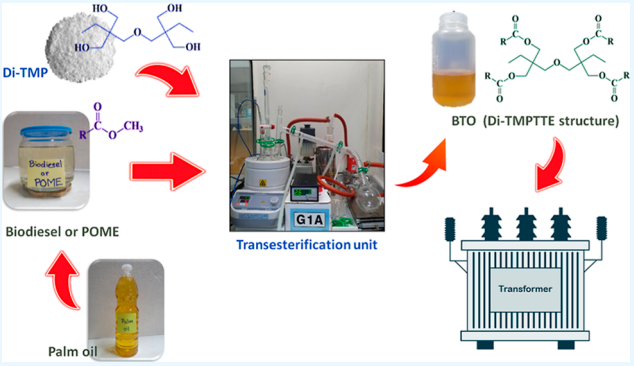

1. INTRODUCTION

The ongoing climate change has largely been caused by the overconsumption of fossil fuels and massive carbon dioxide (CO_2) emissions for centuries. The substitution of electrical power for the conventional combustion of fossil fuels is one solution toward achieving the net-zero CO_2 emission goal. Consequently, the global demand for electricity consumption is expected to continuously increase by 30% in the next decade.[1,2] Thus, a large number of electrical transformers for electricity distribution are required. An electrical transformer generally consists of three parts: a core, windings, and insulating materials, including paper and a transformer oil (TO). The role of the TO is to ensure the dielectric strength of the gaps between active components, in collaboration with solid materials such as paper and pressboard. In addition, TO improves the dielectric strength of the solid insulation and also works as a cooling medium for the transformer.[3] The market size of electrical transformers and TO will likely be expanded by 4.6%/y[4] and 8%/y,[5] respectively, by 2030.

Mineral oil (MO) has been applied as TO since 1890.[6] However, MO is highly flammable (low flash point and fire point), nonbiodegradable, and poisonous.[3,7] Thus, TO derived from biobased hydrocarbons, such as triglyceride-based oils obtained from plants,[6,8] synthetic esters,[9,10] and natural esters including the liquid insulators produced from gas-to-liquid (GTL) technology,[10,11] is expected to replace MO for a higher safety, sustainability, cleanliness, and environmental compatibility.[6,8−11] Among triglyceride-based oils, palm oil (PO) is a key competitor due to its high productivity[12,13] and low price.[14] Moreover, its high flash point (>250 °C) and fire point (>270 °C) give PO a high potential for application as lubricants and synthetic esters.[15] However, the presence of C═C bonds in the triglyceride structure is susceptible to degradation. Similarly, the oxygen atoms in the ester molecules significantly diminish their thermal and hydrolytic stability compared to MO.[16]

These drawbacks can be solved by replacing the glycerol with neo-polyols to form polyol esters (POEs). This technique can provide POEs with a higher molecular chain length and ester branches resulting in the desired properties, such as eco-compatibility with a greater thermal and oxidative stability than the inherent vegetable oils.[17] Moreover, the pour point and cloud point of POEs are dependent on the degree of ester branches. Typically, POEs can be synthesized via ring opening of epoxidized fatty acids, transesterification, and esterification in

Received: June 28, 2024
Revised: September 2, 2024
Accepted: September 23, 2024
Published: October 5, 2024

Table 1. Previous Studies Involving Transesterification of PO Derivatives and Neo-polyols

PO derivatives	neo-polyols	catalyst	conditions	product	results	ref
POME	TMP	0.6 wt % $NaOCH_3$	O/A[a] = 4.0/1.0 T = 120 °C P = 10 mbar, t = 1.5 h SR[b] = 400 rpm	TMPTE	selectivity$_{TMPTE}$ = 73% yield$_{TMPTE}$ = 46 wt %	20
POME	PE	1.19 wt % $NaOCH_3$	O/A = 4.5/1.0 T = 158 °C t = 1 h, SR = 700 rpm	PETTE	selectivity$_{PETTE}$ = 55% yield$_{PETTE}$ = 37.56% FP[c] = 302 °C PP[d] = < − 20 °C	21
high oleic POME	PE	1.25 wt % $NaOCH_3$	O/A = 4.5/1.0 T = 160 °C P = 1 kPa, t = 2 h SR = 900 rpm	PETTE	selectivity$_{PETTE}$ = 54% yield$_{PETTE}$ = 36%	22
palm kernel oil	Di-TMP	1.7 wt % H_2SO_4	O/A = 1.6/1.0 T = 150 °C t = 4.6 h	Di-TMPTTE	selectivity$_{Di\text{-}TMPTTE}$ = 91% yield$_{Di\text{-}TMPTTE}$ = 78% FP = 365 °C PP = −6 °C T_{onset}[e] = 199.7 °C	23

[a]O/A = mole ratio of PO derivatives/neo-polyol. [b]SR = stirring rate. [c]FP = flash point. [d]PP = pour point. [e]Detected by TGA.

the presence of an enzymic, acidic, or basic catalyst.[18,19] Salih et al.[18] prepared POE from the ring opening of epoxidized ricinoleic acid. They observed that the POE having a tetra-ester structure had the lowest pour point and cloud point of ca. −44 and −41 °C, respectively. However, this process required sulfuric acid (H_2SO_4) in the triester and tetra-ester formation step, which could corrode the equipment. Considering esterification and transesterification, the raw materials used in esterification are fatty acids, while transesterification can use either triglyceride or fatty acid methyl esters. These materials are then reacted with neo-polyols to form the POEs.

With the growing trend of electric vehicles, PO methyl ester (POME) as biodiesel will be in excess in the market. Thus, POME is an attractive feedstock for POE production to maintain the biodiesel industry and PO prices as well as to support a clean and sustainable electrification policy. Several forms of POEs derived from the transesterification of POME or PO derivatives and neo-polyols, such as trimethylolpropane (TMP), pentaerythritol (PE), and ditrimethylolpropane (Di-TMP), to obtain the trimethylolpropane triester (TMPTE), pentaerythritol tetra-ester (PETTE), and ditrimethylolpropane tetra-ester (Di-TMPTTE), respectively, are shown in Table 1. Under the given reaction conditions, the use of TMP and PE provided TMPTE and PETTE yields of less than 50 wt %.[20−22] However, the existence of the tetra-ester species increased the flash point of the obtained POEs to 302 °C, so they could be used as lubricants for applications requiring a high resistance to thermal degradation. In the case of Di-TMP, Bahadi et al.[23] reported that the transesterification of palm kernel oil and Di-TMP gave a 78% Di-TMPTTE yield with a high flash point of 365 °C and a quite low pour point of −6 °C. However, this system used H_2SO_4 as the catalyst, which hence required plenty of water for neutralizing the obtained product. This raises not only environmental concerns, but the use of an acid-catalyzed process is rarely commercialized due to ca. 4000 times slower reaction rate than when using a basic catalyst.[24] Normally, the methoxide ion (CH_3O^-) generated from sodium methoxide ($NaOCH_3$) is applied as the catalyst for transesterification to avoid soap formation, which generally occurs in systems catalyzed by hydroxide ions derived from potassium hydroxide or sodium hydroxide.[25]

According to the benefit of using Di-TMP alcohol and a basic catalytic process for the production of POEs as outlined above, this research aimed to prepare a highly stable BTO via transesterification from POME and Di-TMP catalyzed by $NaOCH_3$ and to investigate the optimal conditions (reaction time, catalyst concentration, POME/Di-TMP molar ratio, reaction pressure, reaction temperature, and stirring rate) to provide the highest Di-TMPTTE selectivity. Moreover, the important properties of the obtained BTO, such as its kinematic viscosity, flash point, pour point, oxidation stability, and dielectric breakdown voltage, were reported as a function of the Di-TMP ester portion and compared to a commercial BTO (Envirotemp FR3) and MO. With respect to commercial-scale production, the techno-economic analysis (TEA) of this process was also elucidated.

2. EXPERIMENTAL SECTION

2.1. Materials. The POME and refined-bleached-deodorized PO (RBDPO) were purchased from Patum Vegetable Oil Co., Ltd. (Pathum Thani, Thailand). A commercial BTO under the trade name of "Envirotemp FR3" manufactured by Cargill Industrial Specialties was obtained from a local transformer company in Thailand. The Di-TMP, 99% methyl oleate (MeO), *N*-methyl-*N*-trimethylsilyl trifluoroacetamide (MSTFA) used as the derivatizing agent, GC-grade ethyl acetate, and anhydrous $NaOCH_3$ were purchased from Sigma-Aldrich (Singapore).

2.2. Preparation of BTO via Transesterification of POME and Di-TMP. The procedure for transesterification of POME and Di-TMP was adapted from previous literature.[22,23] The reaction was conducted in a 500 mL three-neck round-bottom flask equipped with a condenser connected to a vacuum pump, a thermocouple, a vacuum screw additional funnel, and a magnetic stirrer bar. A relief valve was installed between the condenser and the vacuum pump to adjust the vacuum pressure to the desired point. This apparatus was then placed in a heating mantle equipped with a stirring mode (Figure S1). The Di-TMP was mixed with 4−8 mol % $NaOCH_3$ based on the Di-TMP content and filled in the vacuum screw addition funnel. The POME/Di-TMP molar ratio was controlled in the range of 4.0/1.0 to 8.0/1.0. After loading the POME into the reactor flask, the pressure and temperature in the reactor were adjusted to 3.5 mbar and 100 °C overnight under an agitation speed of 600 rpm to eliminate moisture in the POME. Before ramping to the desired reaction temperature (140−170 °C), the vacuum pressure of the system was adjusted to the target point (3.5−10.0 mbar) and the mixed solid chemicals (Di-TMP and $NaOCH_3$) were then gradually released from the vacuum screw additional funnel at a feed rate of 0.5 g/min. The reaction was allowed to proceed for 2−12 h under an agitation rate of 200−600 rpm. When the reaction was ceased, the collected liquid product was cooled down to room temperature under vacuum before filtering using Whatman paper no. 1 to separate out the solid residue. The resultant liquid product was then transferred to a rotary evaporator at 180 °C under 0.5 mbar to remove unreacted POME in the BTO before being kept in an amber bottle and stored in a dry place.

2.3. Product Analysis. *2.3.1. Structural Characterization of BTO.* After the evaporation step, the chemical structure of the obtained BTO was characterized using attenuated total

https://doi.org/10.1021/acsomega.4c05987
ACS Omega 2024, 9, 42396−42409

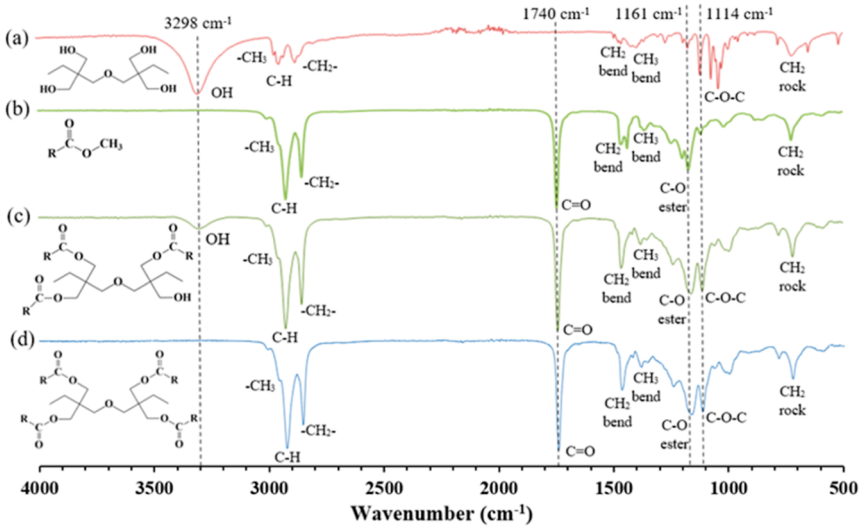

Figure 1. Representative FTIR spectra of (a) Di-TMP, (b) POME, (c) BTO at 61.3% POME conversion (21.0% selectivity to POME-Di-TMPTTE), and (d) BTO at a 90.3% POME conversion (96.6% selectivity to POME-Di-TMPTTE) (where R is the fatty acid chain).

reflectance−Fourier-transform infrared spectroscopy (ATR−FTIR; PerkinElmer Infrared Spectrophotometer) within the range of 500−4000 cm^{-1}. Both ^{1}H- and ^{13}C nuclear magnetic resonance (NMR) analyses were applied to confirm the ATR−FTIR results, using a JEOL-ECP 400 spectrometer at 400 MHz (^{1}H) and 100.61 MHz (^{13}C). Deuterated chloroform ($CDCl_3$) was used as the solvent for POME and BTO, while Di-TMP was dissolved in deuterated methanol (MEOD).

2.3.2. Determination of the Levels of POME Conversion and Selectivity to POME-Di-TMP Esters in BTO. The esters in the obtained crude BTO before evaporation were distinguished as monoester (POME-Di-TMPME), diester (POME-Di-TMPDE), triester (POME-Di-TMPTE), and tetra-ester (POME-Di-TMPTTE) using gas chromatography with a flame ionization detector (GC-FID; GC-2010, Shimadzu) and equipped with a DB-5HT (15 m × 0.320 mm × 0.10 μm) column. The detail of the condition applied for GC-FID analysis is given in Supporting Information A.

Due to the lack of commercial standards for all Di-TMP esters produced in this system, the yield of each Di-TMP ester could not be directly calculated using calibration curves from standard references. To express the amount of ester products, the term "selectivity to ester" was used to represent the fraction of each Di-TMP ester in the resulting BTO. This was calculated from the GC-FID chromatogram as the ratio of the peak area of the specified ester to the total peak area of ester products, as shown in eq 2, assuming that the response factor of each ester was equal. To identify each ester in the obtained BTO, the Di-TMP esters prepared from transesterification of MeO and Di-TMP adapted from a previous research work[23] were used as reference materials in this research. Details on the preparation of MeO-Di-TMP esters (MeO-Di-TMPE) and the range of retention times in the GC-FID chromatogram (Figure B1) used to specify each ester are provided in Supporting Information B. The levels of POME conversion and selectivity to each ester in the obtained BTO were calculated following eqs 1 and 2,[23] respectively

$$\text{POME conversion (\%)} = \left[1 - \frac{n_{\text{unreacted POME}}}{n_{\text{fed POME}}}\right] \times 100 \quad (1)$$

$$\text{selectivity to ester (\%)} = \left(\frac{\text{area of } i_{\text{ester}}}{\sum \text{area of } i_{\text{ester}}}\right) \times 100 \quad (2)$$

where $n_{\text{unreacted POME}}$ (mol) is obtained from the calibration curve of the POME concentration (Figure A1 in Supporting Information A), and $n_{\text{fed POME}}$ (mol) is the initial POME content applied to the system. The average molecular weight (M_w) of POME, calculated from the mass fraction of fatty acids that appeared in POME (Table S1), was ca. 283, and the area of i_{ester} was the peak area of the GC-FID chromatogram for the specified ester (i_{ester}) in the BTO.

2.4. Physical, Electrical, and Thermal Properties of the BTO. The physical and electrical properties of the BTO were attested following The International Electrotechnical Commission 62770 standards (IEC 62770)[26] for evaluation of kinematic viscosity at 40 °C (ISO 3104), flash point (ISO 2719), pour point (ISO 3016), and dielectric breakdown voltage (IEC 60156). The BTO used for these analyses was obtained from an evaporation step to reduce the amount of the unreacted POME to <1 wt %. The oxidation stability of the BTO was also analyzed following the Rancimat method (EN15751) using a Metrohm 743 (Rancimat, Herisau, Switzerland).[27] Briefly, the sample (7.5 g) was added into the Rancimat flask and then analyzed under a controlled airflow rate of 10 L/h at 110 °C. The oxidation stability was then determined from the increasing water conductivity as the induction period (calculated by the Rancimat software) in hours. For the measurement of the dielectric breakdown voltage, the sample was dried in a vacuum oven at 60 °C for 24 h to reduce the water content to below 50 ppm before testing. All analyses were performed in duplicate and reported as the average values.

The thermal degradation temperature of POME and BTO was also measured using thermogravimetric analysis (TGA; TGA/SDTA 851e; Mettler Toledo) at a heating rate of 10 °C/min from 30 to 800 °C under a nitrogen atmosphere at a flow rate of 10 mL/min. The onset (T_{onset}) and the endset (T_{endset}) degradation temperatures were obtained from the intersection of two tangents at the initial and the final stages of the thermogravimetric curve. The maximum decomposition temperature (T_p), reflecting the degradation temperature at the

https://doi.org/10.1021/acsomega.4c05987
ACS Omega 2024, 9, 42396−42409

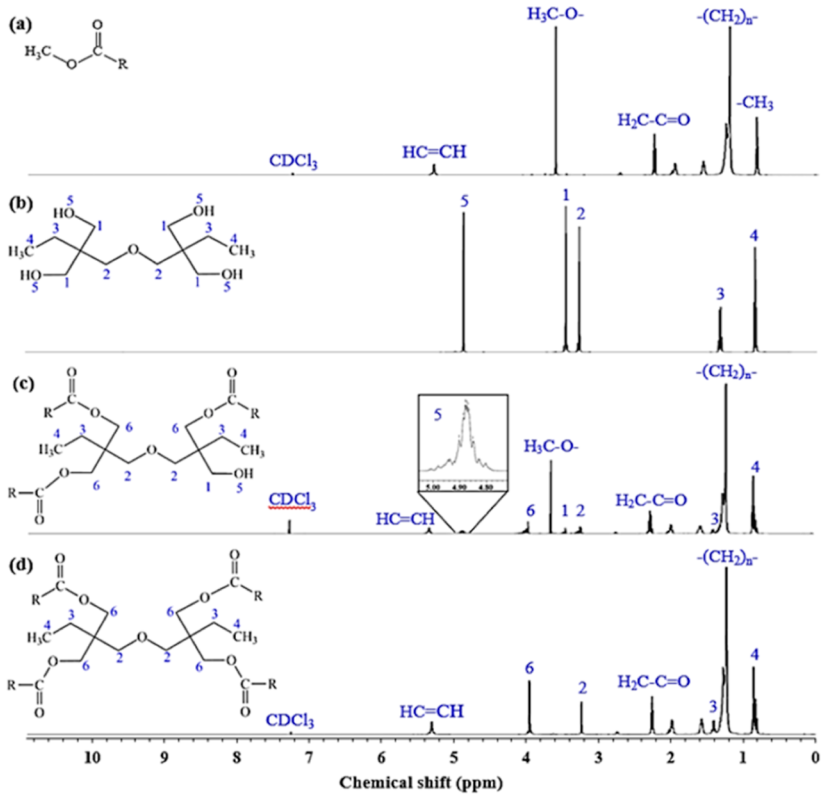

Figure 2. Representative ^{1}H NMR spectra of (a) POME, (b) Di-TMP, (c) BTO at 61.3% POME conversion (21.0% selectivity to POME-Di-TMPTTE), and (d) BTO at 90.3% POME conversion (96.6% selectivity to POME-Di-TMPTTE) (where R is the fatty acid chain).

maximum weight-loss rate, was measured at the peak of the derivative thermogravimetric curve.

2.5. Process Feasibility Assessment Using TEA. The economic viability of the process design was evaluated using TEA. The case exhibiting the optimal condition obtained from Section 2.2 was used as the example for calculating the material and energy balance of the BTO production via transesterification of POME and Di-TMP. The details of material-energy balance, process investment, and operating cost were estimated using the Aspen Plus V9 simulation software with the PENG-ROB property. This method is appropriate for hydrocarbon processing applications. The stoichiometric reactor model was also used for the simulation according to the experimental results. For the other unit operations, the simulation model was selected based on their function under a real process operating condition. When the laboratory-scale model was simulated and validated, the scale-up model was then performed and used to find the process feasibility via TEA. The final obtained result was compared to the commercial BTO price (Envirotemp FR3).

3. RESULTS AND DISCUSSION

3.1. Structural Characterization of BTO. The chemical structure of BTO derived from transesterification of POME and Di-TMP for 2 h at 160 °C and 3.5 mbar with a 5/1 POME/Di-TMP molar ratio and 8 mol % $NaOCH_3$ (based on the Di-TMP content) and constant stirring at 300 rpm was analyzed by ATR−FTIR and ^{1}H- and ^{13}C NMR spectroscopy.

For the FTIR spectra, peaks at 1740 and 1161 cm^{-1}, attributed to C═O (ester carbonyl) and C−O (ester group stretching), respectively,[23] were found in POME (Figure 1b) and BTO (Figure 1c ,d). Moreover, the FTIR spectra of BTO indicated a new peak at 1114 cm^{-1} assigned to C−O−C aliphatic ether,[28] which was also found in the Di-TMP structure (Figure 1a). It was observed that the peak of the hydroxyl group associated with the Di-TMP structure at 3298 cm^{-1} in BTO became smaller as the POME conversion level reached 61.3% and eventually disappeared at a 90.3% POME conversion level with a 96.6% selectivity toward POME-Di-TMPTTE. This indicated the complete consumption of Di-TMP during transesterification, leading to the production of BTO as POME-Di-TMPTTE.

The chemical structures of POME and BTO obtained from the same reaction conditions as described above were also examined by ^{1}H NMR and ^{13}C NMR (Figures 2 and 3). In Figure 2a, the ^{1}H NMR spectra of POME show the characteristic peaks at 3.63 and 2.27 ppm attributed to the protons in the methoxy group (CH_3−O−) and the methylene protons of −CH_2−C═O, respectively. Moreover, chemical shifts at 5.25 ppm, assigned to the olefinic proton (−C═C−H), and at 1.4−1.6 ppm, which corresponded to the proton of the methylene group [-$(CH_2)_n$−] in the POME structure, were observed.[23] Figure 2b exhibits the ^{1}H NMR spectra of Di-TMP, which showed characteristic peaks at 3.5, 3.3, 1.4, 0.8, and 4.8 ppm that correspond to the protons of −H_2C−OH (1), −H_2C−O−CH_2− (2), −C−CH_2−C− (3), −CH_3 (4), and −OH (5), respectively. After transesterification, the ^{1}H NMR spectra of the obtained BTO with a 61.3% POME conversion level (Figure 2c) showed a new peak at 3.97 ppm, which corresponds to the protons of −H_2C−O−C− (6), whereas the intensities of the peaks at 3.5 and 4.8 ppm were smaller. This indicated that the hydroxyl group (−OH) of Di-TMP was reacted with POME to form ester (−O−C═O).[29] When the level of POME conversion reached 90.3%, the ^{1}H NMR spectra of the obtained

https://doi.org/10.1021/acsomega.4c05987
ACS Omega 2024, 9, 42396−42409

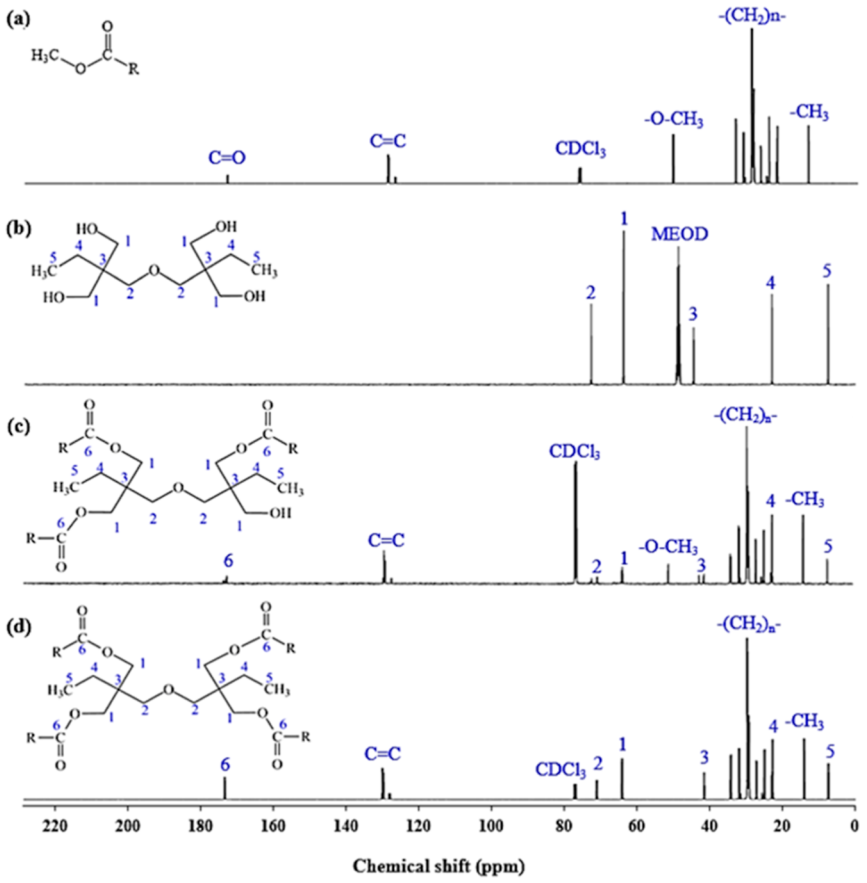

Figure 3. Representative ^{13}C NMR spectra of (a) POME, (b) Di-TMP, (c) BTO at 61.3% POME conversion (21.0% selectivity to POME-Di-TMPTTE), and (d) BTO at 90.3% POME conversion (96.6% selectivity to POME-Di-TMPTTE) (where R is the fatty acid chain).

BTO with 96.6% Di-TMPTTE selectivity (Figure 2d) showed higher peak intensities at 5.25, 3.97, and 2.27 ppm that correspond to −C═C−H, $-CH_2-C{=}O$, and $-H_2C-O-C$, respectively, with disappearance of the peaks at 3.5 and 4.8 ppm. This suggested that the hydroxyl groups in Di-TMP were completely reacted with POME to produce POME-Di-TMPTTE.[29]

The ^{13}C NMR spectra of the obtained BTO showed that the peak at 51.2 ppm attributed to $-O-CH_3$[30] in POME (Figure 3a) became smaller (Figure 3c) and disappeared (Figure 3d) when the level of the POME conversion increased. Figure 3b depicts the signals at 72 (2), 64 (1), 42.9 (3), 22 (4), and 7.2 ppm (5) assigned to C−O−C, $-H_2C-O$, quaternary carbon, $-CH_2-$, and $-CH_3$, respectively, which belonged to Di-TMP. After transesterification, the signals at 72 and 42.9 ppm of C−O−C and quaternary carbon in Di-TMP were shifted to 71 and 41.5 ppm, respectively, in the obtained BTO (Figure 3c,d). Moreover, the peak intensity of the carbon ester carbonyl (C═O) located at 173.5 ppm (6) in BTO was higher. The formation of these peaks indicated the successful transesterification of POME and Di-TMP to form the ester-based BTO.

The POME conversion level and selectivity to each ester (POME-Di-TMPME, POME-Di-TMPDE, POME-Di-TMPTE, and POME-Di-TMPTTE) in the BTO were quantified by GC-FID chromatography (Figure 4). The BTO was prepared via transesterification at 160 °C using a 5.0/1.0 POME/Di-TMP molar ratio and 8 mol % $NaOCH_3$ (based on the Di-TMP content) under 3.5 mbar for 1 and 2 h. Before transesterification, the GC chromatograms of POME and Di-TMP showed their characteristic peaks at a retention time in the range of 2−16 min (Figure 4a) and 10.4 min (Figure 4b), respectively. After the reaction, the GC chromatogram of the BTO obtained from 1 h reaction time (Figure 4c) showed the existence of unreacted POME with the disappearance of Di-TMP. This suggested that Di-TMP was completely reacted with POME to generate BTO containing various POME-Di-TMP esters. The above condition resulted in a 61.3% POME conversion level with a 52.4% POME-Di-TMPTE selectivity as the dominant ester product in the obtained BTO. The lower amount of Di-TMPTTE produced reflected the effect of steric hindrance of the POME-Di-TMPTE structure, which inhibited the reaction with new POME molecules to form POME-Di-TMPTTE.[22] When the reaction time was increased to 2 h, a 90.3% POME conversion level with a remarkably higher POME-Di-TMPTTE selectivity of 96.6% was obtained with smaller peaks of unreacted POME and POME-Di-TMPTE (Figure 4d). The peaks of POME-Di-TMPME and POME-Di-TMPDE also disappeared from the obtained BTO structure.

3.2. Effect of Reaction Parameters on Levels of POME Conversion and Ester Selectivity. To investigate the effect of the reaction parameters used in the transesterification of POME and Di-TMP on the POME conversion level and the selectivity to different esters in the obtained BTO, six important parameters, the reaction time, catalyst dosage, POME/Di-TMP molar ratio, reaction temperature, reaction pressure, and stirring rate, were explored.

3.2.1. Effect of the Reaction Time and Proposed Reaction Mechanism. The mechanism of transesterification of POME

https://doi.org/10.1021/acsomega.4c05987
ACS Omega 2024, 9, 42396−42409

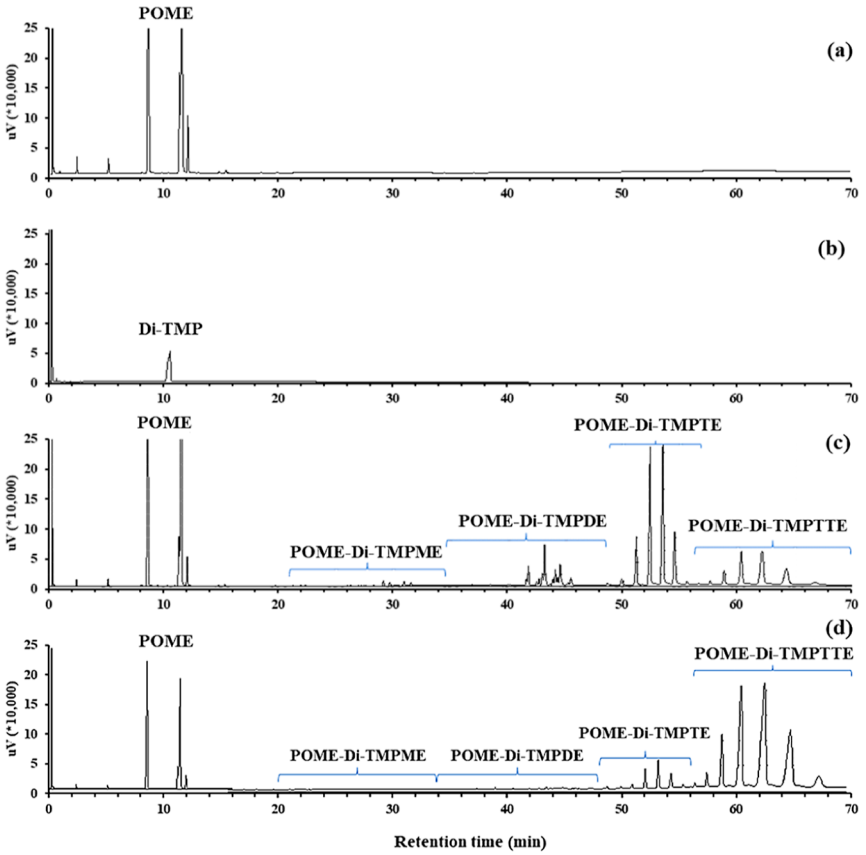

Figure 4. Representative GC-FID chromatograms of (a) POME, (b) Di-TMP, and BTO obtained from a reaction time of (c) 1 h (61.3% POME conversion with 21.0% selectivity to POME-Di-TMPTTE) and (d) 2 h (90.3% POME conversion with 96.6% selectivity to POME-Di-TMPTTE).

and Di-TMP was proposed through the reaction time when the system was operated in the presence of a 4.5/1.0 POME/Di-TMP molar ratio and 4 mol % $NaOCH_3$ (based on the Di-TMP content) under 5 mbar and a 300 rpm stirring rate at 160 °C. Samples were collected at the given time intervals (15 min−12 h). The results in Figure 5 showed that the POME conversion level increased to 75% within the first 15−60 min of the reaction course and then gradually increased to 93% at 6−8 h onward.

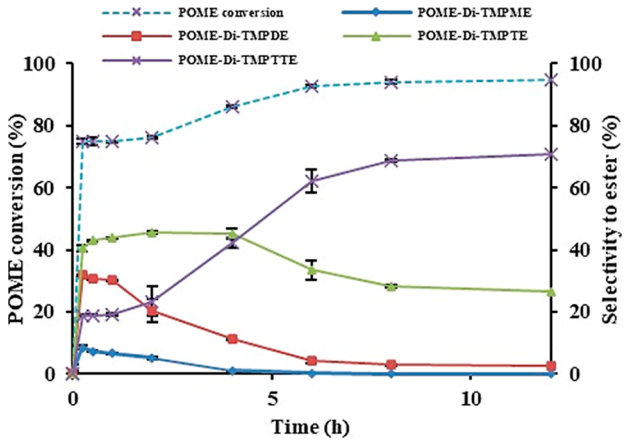

Figure 5. Profiles of the POME conversion and selectivity to esters in the BTO obtained from transesterification of POME and Di-TMP (condition: POME/Di-TMP molar ratio = 4.5/1.0; $NaOCH_3$ content = 4 mol % (based on Di-TMP), stirring rate = 300 rpm, pressure = 5 mbar, and temperature = 160 °C).

For the selectivity to each ester, POME-Di-TMPTE was the main product over the first hour (44%) followed by POME-Di-TMPDE (ca. 31%) and POME-Di-TMPTTE (<19%) with a very low selectivity of POME-Di-TMPME (<10%). The selectivity to POME-Di-TMPTE was slightly increased to 45% after 4 h and then declined to less than 27% at longer reaction times of 8−12 h. During the same period, the POME-Di-TMPTTE selectivity increased and reached almost the same selectivity as that for POME-Di-TMPTE (42%) at 4 h. It then became the dominant fraction in the product and attained 70% selectivity when the reaction time was 8−12 h. In contrast, the selectivity to POME-Di-TMPDE and POME-Di-TMPME declined to <3% at 8 and 4 h, respectively.

According to the information presented above and that in the previous literature,[20] the reaction mechanism for the transesterification of POME and Di-TMP in the presence of the $NaOCH_3$ catalyst is proposed in Figure 6. This system was first activated by the reaction of Di-TMP and $NaOCH_3$ to form Di-TMP alkoxide (Di-TMP ion) and methanol. The Di-TMP alkoxide then reacted with the carbonyl group of POME to instantaneously produce POME-Di-TMPME as the first intermediate and release $NaOCH_3$, which subsequently reacted with Di-TMP again.[20] Further, POME molecules would then replace the existing hydroxyl groups in the POME-Di-TMPME structure, following the same procedure, to sequentially form POME-Di-TMPDE, POME-Di-TMPTE, and last POME-Di-TMPTTE. The reactions that occurred in this system are presented in eqs 3−6

$$\text{Di-TMP} + 1\text{POME} \leftrightarrow \text{POME-Di-TMPME} + 1\text{MeOH} \quad (3)$$

https://doi.org/10.1021/acsomega.4c05987
ACS Omega 2024, 9, 42396−42409

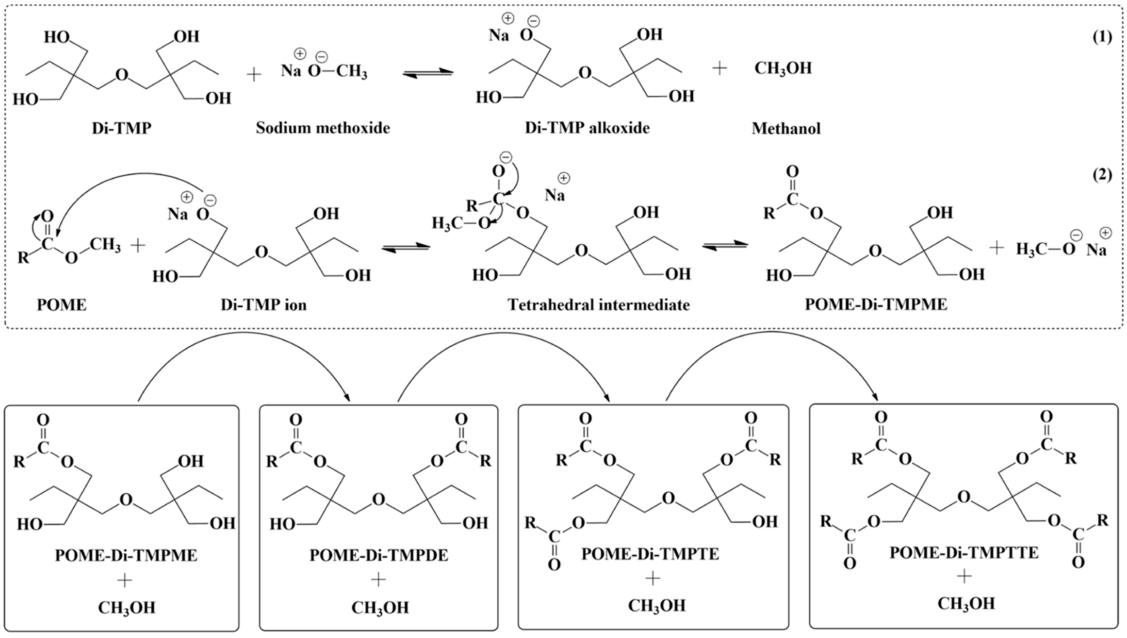

Figure 6. Proposed transesterification mechanism of POME and Di-TMP to form POME-Di-TMP esters (where R is the fatty acid chain).

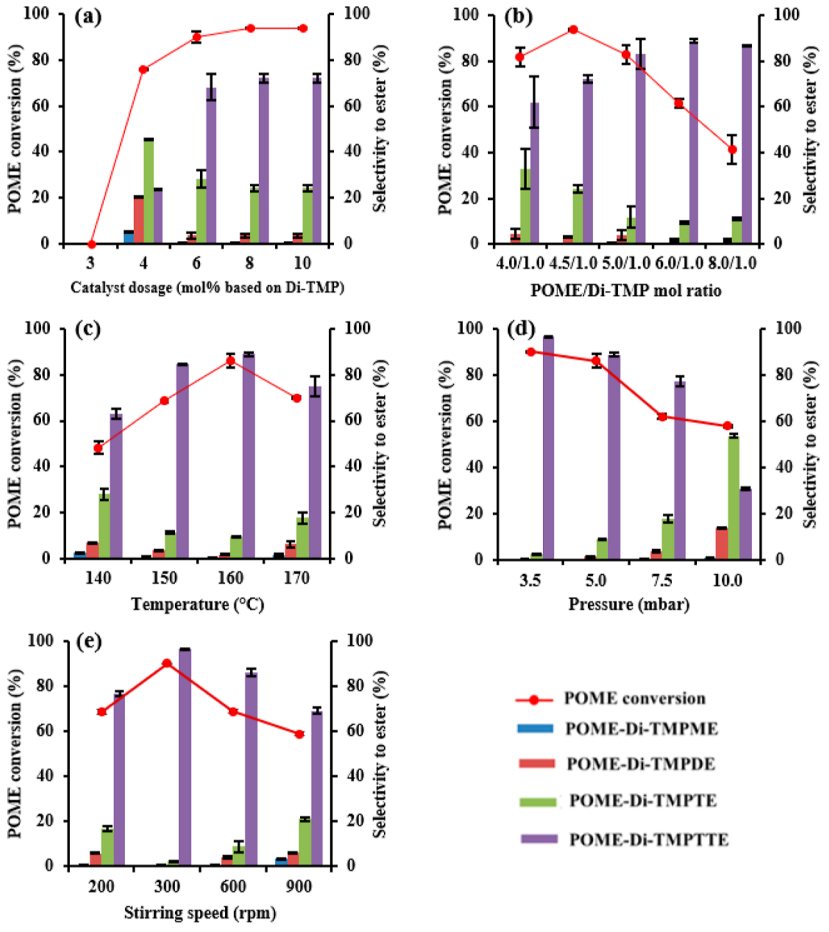

Figure 7. Effects of the (a) catalyst dosage, (b) POME/Di-TMP molar ratio, (c) reaction temperature, (d) reaction pressure, and (e) stirring speed on the level of POME conversion and selectivity to Di-TMP esters in the BTO prepared transesterification of POME and Di-TMP for 2 h.

$$\text{POME-Di-TMPME} + 1\text{POME} \leftrightarrow \text{POME-Di-TMPDE} + 1\text{MeOH} \quad (4)$$

$$\text{POME-Di-TMPDE} + 1\text{POME} \leftrightarrow \text{POME-Di-TMPTE} + 1\text{MeOH} \quad (5)$$

https://doi.org/10.1021/acsomega.4c05987
ACS Omega 2024, 9, 42396−42409

POME-Di-TMPTE + 1POME
↔ POME-Di-TMPTTE + 1MeOH (6)

Since the 2 h reaction time was the initial point to enhance the POME-Di-TMPTTE selectivity in the obtained BTO (Figure 5), this reaction time was selected for further studies on the effects of the other parameters on the POME conversion level and selectivity to each ester (Figure 7).

3.2.2. Effect of the Catalyst Dosage. The effect of the $NaOCH_3$ catalyst dosage (3−10 mol % based on the Di-TMP content) on the transesterification of POME and Di-TMP is shown in Figure 7a. The reaction was conducted for 2 h at 160 °C by using a 4.5/1.0 POME/Di-TMP molar ratio under 5 mbar with a stirring speed of 300 rpm. The use of 3 mol % $NaOCH_3$ (based on the Di-TMP content) was insufficient to activate the reaction. Increasing the $NaOCH_3$ content to 4 mol % markedly enhanced the level of POME conversion to 76.0%, but the POME-Di-TMPTTE selectivity was only 23.5%. Thereafter, both the POME conversion level and POME-Di-TMPTTE selectivity increased when increasing the catalyst dosage to 8 mol %, giving a POME conversion level and a POME-Di-TMPTTE selectivity of 94.2% and 72.1%, respectively, and then leveled off when a 10 mol % $NaOCH_3$ catalyst dosage was applied. This reflects that 10 mol % $NaOCH_3$ was excessive and so gave no improvement in the POME conversion level and POME-Di-TMPTTE selectivity due to the steric hindrance of the produced intermediates.[22] Thus, the appropriate catalyst content provided a sufficient concentration of Na^+-OCH_3 to facilitate the formation of Di-TMP alkoxide, which reacted with POME to produce Di-TMP esters as proposed in the reaction mechanism shown in Figure 6. Herein, an 8 mol % $NaOCH_3$ catalyst dosage (based on Di-TMP content) or 0.27 wt % based on the POME content was deemed to be optimal even though it was less than that used in previous studies for producing tetra-esters. For example, Bahadi et al.[23] used 1.7 wt % H_2SO_4 for the acid-catalyzed transesterification of crude palm kernel oil and Di-TMP to give a 79% yield and 91% selectivity of the tetra-ester. Idrus et al.[22] applied 1.25 wt % $NaOCH_3$ for the preparation of PE tetraoleate esters via transesterification of POME and PE.

3.2.3. Effect of the POME/Di-TMP Molar Ratio. The molar ratio of reactants is one of the important parameters affecting transesterification.[31,32] From the overall process, the stoichiometric POME/Di-TMP molar ratio was 4.0/1.0. However, an excess amount of POME could enhance the forward reaction and hinder the backward reaction.[32] In this research, the effect of the POME/Di-TMP molar ratio on the POME conversion level and selectivity to POME-Di-TMP esters was evaluated over a range from 4.0/1.0 to 8.0/1.0 (Figure 7b). The reaction was performed at 160 °C, 5 mbar, and an agitation rate of 300 rpm for 2 h in the presence of 8 mol % $NaOCH_3$ (based on Di-TMP content). When the stoichiometric POME/Di-TMP molar ratio was 4.0/1.0, the levels of POME conversion and POME-Di-TMPTTE selectivity were 82% and 62%, respectively. These values were then improved to 94% and 83%, respectively, when the POME/Di-TMP molar ratio was slightly increased to 4.5/1.0 and 5.0/1.0, respectively, suggesting that the higher POME content promoted the forward reaction following Le Châtelier's principle.[33] Above this point, the POME conversion level decreased to 41% when the POME/Di-TMP molar ratio was 8.0/1.0 due to the excessive POME content providing a high amount of unreacted POME in the system. However, the high selectivity to POME-Di-TMPTTE remained at ca. 87%. To achieve a high POME conversion level and selectivity to POME-Di-TMPTTE in the produced BTO, the optimal POME/Di-TMP molar ratio was thus selected as 5.0/1.0 for further study.

3.2.4. Effect of the Reaction Temperature. To avoid Di-TMP sublimation (215 °C) and POME vaporization (180 °C),[22] the reaction temperature was varied in the range of 140−170 °C to study its influence on the transesterification of POME and Di-TMP. The other reaction parameters were kept constant at a 5.0/1.0 POME/Di-TMP molar ratio, 8 mol % $NaOCH_3$ based on the Di-TMP content, 5 mbar, and a 300 rpm stirring rate for 2 h. Increasing the reaction temperature from 140 to 160 °C enhanced the POME conversion level and POME-Di-TMPTTE selectivity from 48.1% to 86.1% and from 63% to 89%, respectively (Figure 7c). However, they were both drastically decreased when the reaction temperature was further increased to 170 °C due to the partial vaporization of POME, which was removed together with the methanol from the system. This result was consistent with previous reports on the preparation of PE tetraoleate esters via transesterification of POME and PE[22] and the transesterification of POME and TMP for producing Di-TMPTE.[34,35]

3.2.5. Effect of the Vacuum Pressure. To avoid the backward reaction (eqs 3−6) due to the buildup of methanol generated during the reaction, the transesterification of POME and Di-TMP needs to be performed under low pressure. Thus, the effect of the vacuum pressure on the transesterification was evaluated by controlling the vacuum pressure in the range of 3.5−10.0 mbar. The POME/Di-TMP molar ratio and the $NaOCH_3$ content were kept constant at 5.0/1.0 and 8 mol % based on the amount of Di-TMP, respectively, and the reaction was operated at 160 °C for 2 h under 300 rpm agitation. The results (Figure 7d) indicated that the highest POME conversion level (90.3%) and POME-Di-TMPTTE selectivity (96.6%) were obtained at 3.5 mbar. Above this point, both values tended to decrease and reached a 58% POME conversion level and a 31% POME-Di-TMPTTE selectivity when the system was operated at 10 mbar. Thus, a low operating pressure was important to eliminate the methanol and so prevent the backward reaction between methanol and POME-Di-TMP esters.[22,34,36] Therefore, the optimum pressure of 3.5 mbar was selected for the transesterification of POME with Di-TMP operated at 160 °C.

3.2.6. Effect of the Stirring Rate. The proper mixing of the solid Di-TMP to be well dissolved in the POME phase is essential to obtain a homogeneous solution for inducing molecular interactions among the reactants in the given reaction time.[35] Accordingly, the stirring speed played an important role in accelerating the reaction. At 160 °C for 2 h and 3.5 mbar in the presence of 5.0/1.0 POME/Di-TMP molar ratio and 8 mol % $NaOCH_3$ based on the Di-TMP content, Figure 7e shows that increasing the agitation rate from 200 to 300 rpm significantly enhanced the POME conversion level and POME-Di-TMPTTE selectivity in the obtained BTO from 68.6% to 90.3% and from 76.7% to 96.6%, respectively. This was due to the increased contact between POME and Di-TMP resulting from a homogeneous mixture.[37] However, increasing the stirring rate further to 900 rpm decreased both the POME conversion level and POME-Di-TMPTTE selectivity to 58.8% and 69.3%, respectively. It was possible that the severe stirring rate created turbulent mixing, which decreased the mixing efficiency due to the higher inertial-convective mixing effect.[38]

3.3. Properties of the Prepared BTO. Since the BTO prepared from the transesterification of POME and Di-TMP was expected to replace the conventional MO used in electrical

https://doi.org/10.1021/acsomega.4c05987
ACS Omega 2024, 9, 42396−42409

Table 2. Comparative Properties of POME, FR3, MO, and BTO Containing Different Proportions of POME-Di-TMP Esters

property	testing method	limited value[a]	POME	proportion of esters in BTO[b]				FR3	MO
				0/10/20/70	0/4/16/80	0/1/9/90	0/1/2/97		
oxidation stability (h)	EN15751		14.3	13.0	18.7	24.3	49.6	13.9	168
breakdown voltage (kV)	IEC 60156	≥50	32.7	95	97	100	100	81.3	67.9
flash point (°C)	ISO 2719	≥250	180	238	242	254	310	252	150
kinematic viscosity at 40 °C (mm^2/s)	ISO 3104	≤50	4.46	94.9	95.3	95.7	96.7	33.2	8.1
pour point (°C)	ISO 3016	<−10	12	10	16	17	17	−20	−40

[a]Following the IEC 62770 standard, except for the oxidation stability, we used the Rancimat method for evaluation. [b]Proportion of esters = POME-Di-TMPME/POME-Di-TMPDE/POME-Di-TMPTE/POME-Di-TMPTTE.

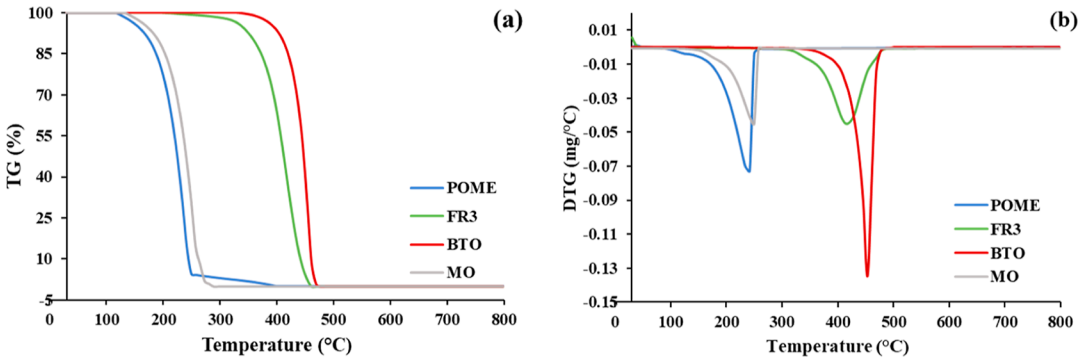

Figure 8. Comparative (a) TG and (b) DTG curves of POME, FR3, MO, and BTO (POME-Di-TMPME/POME-Di-TMPDE/POME-Di-TMPTE/POME-Di-TMPTTE = 0/1/2/97).

transformers, several properties of the obtained BTO were measured according to the IEC 62770 standard (the kinematic viscosity at 40 °C), flash point, pour point, and dielectric breakdown voltage—as a function of the POME-Di-TMP esters in the obtained BTO (POME-Di-TMPME/POME-Di-TMPDE/POME-Di-TMPTE/POME-Di-TMPTTE = 0/10/20/70, 0/4/16/80, 0/1/9/90, and 0/1/2/97), with the results shown in Table 2. Moreover, the oxidation stability was evaluated by the Rancimat method and is reported in Table 2. These properties were compared to those of the commercial BTO (FR3) and MO.

The oxidation stability is an important property to determine the degree of oxidation resistance of lubricants. Generally, the ester group has a high resistance to oxidation, so its presence can enhance the stability of the adjacent carbon atoms.[39] The oxidation stability of POME (14.3 h) was improved after transesterification and depended on the proportion of POME-Di-TMPTTE in BTO (Table 2). It was observed that BTO containing the POME-Di-TMPTTE fraction above 70 wt % showed greater oxidation stability than the commercial FR3 (13.9 h). The oxidation stability of BTO increased with an increasing proportion of POME-Di-TMPTTE. The maximum oxidation stability (49.6 h) was found when BTO had a POME-Di-TMPTTE portion of 97 wt %. Thus, the obtained BTO with a lower content of −OH groups was more difficult to oxidize to carboxylic acid.[40] The synthesized BTO also mainly consisted of C16:0 and C18:1 as the major structures at 43.6 and 39.6 wt %, respectively (Table S1). These long-chain fatty acids formed a high ester linkage in the POME-Di-TMPTTE structure, and their saturated composition led to superior oxidation stability.[16,39] In the case of FR3, it is derived from soybean oil[41] and contains C18:2 as the main composition (52.0 wt %) and 83.1 wt % unsaturated composition (Table S1). According to the higher degree of unsaturation of FR3, it was easily deteriorated by oxidation to form free radicals,[16,42] which resulted in its lower oxidation stability than the as-prepared BTO of this study. However, the oxidation stability of MO was much higher at 168 h (Table 2) since its structure generally consists of paraffin, naphthenic, and cyclic hydrocarbons,[3,6,7] which impart high oxidation stability.

The thermal stability of BTO was also investigated using TGA and compared with that of MO, POME, and FR3 (Figure 8 and Table 3). The T_{onset}, T_{endset}, and T_p of POME were 199, 244, and 237 °C, respectively. After transesterification with Di-TMP, the obtained BTO with POME-Di-TMPME/POME-Di-TMPDE/POME-Di-TMPTE/POME-Di-TMPTTE at 0/1/2/97 showed improved thermal decomposition temperatures of 434, 460, and 454 °C for T_{onset}, T_{endset}, and T_p, respectively, due to its higher M_w structure.[43] These thermal decomposition temperatures of BTO were higher than those of FR3 and MO, reflecting that the synthesized BTO was more thermally stable than FR3 and MO due to the absence of β-hydrogen in the polyol esters of BTO.[23] This implied that BTO containing a high POME-Di-TMPTTE proportion could be applied in warm regions.

Table 3. Thermal Degradation Temperature of POME, FR3, MO, and BTO

sample	thermal degradation temperature (°C)		
	T_{onset}	T_{endset}	T_p
POME	199	244	237
BTO[a]	434	460	454
FR3	376	446	415
MO	207	259	253

[a]Portion of esters = POME-Di-TMPME/POME-Di-TMPDE/POME-Di-TMPTE/POME-Di-TMPTTE = 0/1/2/97.

Dielectric breakdown voltage is another important electrical property for evaluating the tolerance level of a lubricant to an electrical charge. A high dielectric breakdown voltage is required

https://doi.org/10.1021/acsomega.4c05987
ACS Omega 2024, 9, 42396−42409

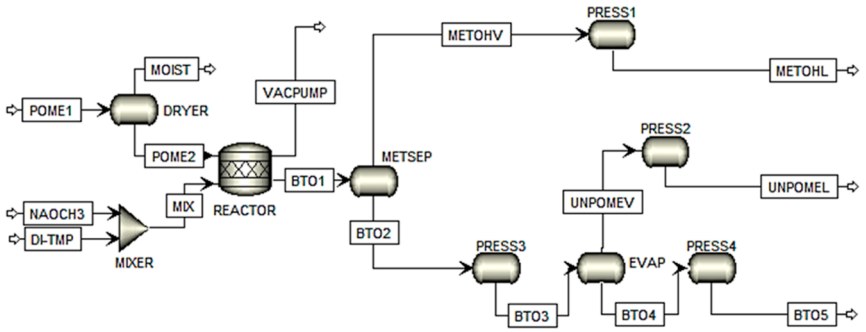

Figure 9. Process flowsheet developed in Aspen Plus V9 for the transesterification of POME and Di-TMP.

to allow safe operation. This value is dependent on the amount of moisture in the lubricant, where an increasing moisture level reduces the dielectric breakdown voltage.[8] According to the IEC 62770 standard, the dielectric breakdown voltage of the liquid insulator used in transformers should be higher than 50 kV. However, the dielectric breakdown voltage of POME was only 32.7 kV, and so it could not be directly applied as a TO without any modification. After transesterification of POME with Di-TMP, the obtained BTO containing various POME-Di-TMPTTE contents had a dielectric breakdown voltage in the range of 95−100 kV, above the minimum requirement according to the IEC 62770 standard and even higher than that for FR3 (81.3 kV) and MO (67.9 kV). The higher dielectric breakdown voltage of the obtained BTO with a higher ester structure reflected the higher resistance against the moisture content.[8]

The flash point is the lowest temperature at which a liquid forms a vapor in the air near its surface before ignition when exposed to an open flame. Thus, a high flash point is required for safe operation with a minimum volatilization at the maximum operating temperature.[44] According to the IEC 62770 standard, the flash point of liquid insulators for use in a transformer should be above 250 °C. Without modification, POME had a flash point at 180 °C, which was lower than the specification. However, after transesterification of POME with Di-TMP, the flash point of the obtained BTO increased to within the range of 238−310 °C as the proportion of POME-Di-TMPTTE in the BTO increased from 70 to 97 wt % (Table 2). This was due to the higher M_w and the number of ester groups in the BTO.[45] At a 90 wt % POME-Di-TMPTTE proportion, the flash point of the BTO was higher than that for FR3 (252 °C) and MO (150 °C). The BTO with higher contents of POME-Di-TMPDE and POME-Di-TMPTE fractions had lower flash points due to the weaker intermolecular bonding that resulted in the easier vaporization of smaller molecules.[43,45]

The properties in terms of pour point and kinematic viscosity reflect the molecular structure of materials.[45] The pour point and kinematic viscosity at 40 °C of POME were 12 °C and 4.46 mm^2/s, respectively, as seen in Table 2. These values were dramatically increased to 17 °C and 96.7 mm^2/s, respectively, after transesterification with Di-TMP to provide the BTO containing 97 wt % POME-Di-TMPTTE. However, these properties were over the upper limitation of the IEC 62770 standard (the pour point and kinematic viscosity at 40 °C should be less than −10 °C and 50 mm^2/s, respectively). This was due to the high degree of saturation and the large molecules of POME-Di-TMPTTE, which could induce stronger covalent intermolecular attractive forces between the fatty acid chains. This led to easier crystallization and higher flow resistance of BTO. In contrast to the prepared BTO, the pour point and kinematic viscosity at 40 °C of FR3 were −20 °C and 33.2 mm^2/s, respectively, meeting the IEC 62770 specification. This was due to its higher total unsaturation level (83.09 wt %; Table S1), where cis double bonds in C18:2 and C18:3 prevent the tight packing together of the fatty acid chains.[46] In the case of MO, its pour point (−40 °C) and kinematic viscosity (8.1 mm^2/s) were qualified for IEC 62770 because it contained medium-chain-length hydrocarbons in a branch or cyclic structure.[3,6,7] Thus, these properties of the BTO derived from transesterification of POME and Di-TMP need further improvement to reduce the flow resistance and so result in higher heat dissipation in electrical transformers during operation. Based on the properties shown in Table 2, the prepared BTO from this system could potentially be applied in the transformers used in warm regions according to its high viscosity and pour point. To apply BTO across all areas, the cold flow properties of the prepared BTO derived from transesterification of POME and Di-TMP may be improved by blending MO and prepared BTO at an appropriate MO/BTO ratio to achieve the desired properties.[47] Additionally, the cold flow improver additives or nanoparticles, such as polymethyl acrylate and titanium dioxide, can be applied to further improve the cold flow properties of BTO.[48,49]

3.4. Evaluation of the Process Feasibility Using TEA.

The TEA and process feasibility for transesterification of POME with Di-TMP to produce BTO at a laboratory scale was evaluated using the Aspen Plus V9 simulation software. The material and energy balance of this process was calculated under the following assumptions: (1) raw material quantities were determined based on laboratory-scale data; (2) the reaction was operated under the optimal condition (5.0/1.0 POME/Di-TMP molar ratio in the presence of 8 mol % $NaOCH_3$ based on the Di-TMP content under 3.5 mbar and 160 °C with a stirring rate of 300 rpm for 2 h to achieve a 90.3% POME conversion with a 96.6% selectivity to POME-Di-TMPTTE); (3) the duration of each batch in the entire BTO production process was 6 h (4 batch/d); and (4) a complete Di-TMP conversion was applied.

The simplified process flow diagram illustrating BTO production at the laboratory scale is depicted in Figure S2. The process involved drying POME in a dryer (DRYER) at 0.1 bar and 100 °C to remove moisture. The dehydrated POME was then fed to a stirring reactor (REACTOR). After mixing the Di-TMP and $NaOCH_3$ catalyst in a screw mixer (MIXER), they were transferred into the REACTOR and transesterification was activated at 160 °C under 3.5 mbar for 2 h to produce BTO. A vacuum pump was also connected to the REACTOR to eliminate the methanol generated during the reaction. The trace of unreacted POME in the obtained BTO was separated using an evaporator operated under 3.5 mbar at 200 °C. Using the

https://doi.org/10.1021/acsomega.4c05987
ACS Omega 2024, 9, 42396−42409

previously detailed assumptions, the overall process diagram for simulating the mass and energy requirements of this process is shown in Figure 9 and summarized in Tables 4 and 5,

Table 4. Comparative Mass Balance between Experimental and Simulated Data

stream	mass flow (g/d)		difference (%)
	simulation	experiment	
BTO1	257.5		
BTO2	235.8		
BTO3	235.8	235.4	0.17
BTO4	211.3		
BTO5	211.3	211.6	0.12
DI-TMP	40.0	40.0	0.00
METOHL	21.7		
METOHV	21.7		
MIX	40.7		
MOIST	2.0		
NAOCH3	0.7	0.69	0.23
POME1	218.9	216.6	1.03
POME2	216.8		
UNPOMEL	24.5	24.1	1.43
UNPOMEV	24.5		

Table 5. Energy Consumption in Each Unit Used in the Transesterification of POME and Di-TMP Evaluated Using Aspen Plus V9

unit	duty (kJ/d)
DRYER	38.4
EVAP	65.8
METSEP	29.1
MIXER	0.00
PRESS1	0.00
PRESS2	0.00
PRESS3	0.00
PRESS4	0.00
REACTOR	139.4

respectively. The resulting BTO, methanol, and unreacted POME were assumed to be collected at atmospheric pressure in the open vessels named PRESS4, PRESS1, and PRESS2, respectively.

A comparison of the mass balance results obtained from the experimental and simulated data (Table 4) revealed a difference of less than 2% in all streams, confirming the validity of the simulation in estimating the process. To assess the energy consumption in each piece of equipment, the simulation results (Table 5) revealed that the REACTOR consumed the highest amount of energy at 139.4 kJ/d, followed by EVAP (65.8 kJ/d), DRYER (38.4 kJ/d), and METSEP (29.1 kJ/d). Meanwhile, the MIXER, used for preparing the Di-TMP and $NaOCH_3$ solid mixture, and the pressurized vessels (PRESS1−PRESS4) were categorized as energy-unconsumed equipment at the laboratory-scale stage.

The process capacity was then scaled up to evaluate the feasibility for commercialization. The TEA for BTO production via transesterification of POME and Di-TMP was conducted using the Aspen Plus V9 software, guided by the following assumptions: (1) a BTO production capacity of 10,000 tons/y; (2) the BTO plant was assumed to operate 300 days/y for 20 y; (3) all chemical costs, such as raw materials, catalysts, and products, were in USD (Table 6); (4) the selling price of the BTO product was the same as that of Envirotemp FR3; (5) the process was conducted at the optimal operating condition as described earlier; and (6) the complete conversion of Di-TMP was assumed. These assumptions facilitated the estimation of mass streams in each piece of equipment, as depicted in Figure 9 and detailed in Table S2. Economic data were thoroughly evaluated and are summarized in Table 7. The primary expenses consisted of operating costs, followed by raw material costs and capital costs, accounting for 14.78%, 15.74%, and 5.15% of the product selling price, respectively. The total cost was 36.65%, while the marginal profit was 63.35% based on setting the product's sale price to be the same as that for Envirotemp FR3. The cost of utilities contributed only ca. 0.06%, indicating that energy consumption was not the primary cost determinant. The TEA estimated an investment return rate of 20%/year, with a payout period of 3.23 y. Consequently, the production of BTO via the transesterification of POME and Di-TMP demonstrates the feasibility for commercialization. However, the other costs, such as the maintenance and replacement costs, were not accounted for in this study, and these will lower the profit of the production process.

Table 6. Comparison of Chemicals and Electricity Costs for BTO Production vs Envirotemp FR3 Price

item	price	source
Chemicals		
POME	1120 USD/ton	50
Di-TMP	5000 USD/ton	51
$NaOCH_3$	2500 USD/ton	52
methanol	360 USD/ton	53
commercial BTO (Envirotemp FR3)	14,400 USD/ton	54
Utility		
electricity	0.15 USD/kW h	55

Table 7. Economic Data of the Simplified Process for BTO Production via Transesterification of POME and Di-TMP

economic information	value
total product sales (USD/y)	131,731,000
total cost	
total operating cost (USD/y)	19,473,288 (14.78%)[a]
total raw materials cost (USD/y)	20,734,400 (15.74%)
total capital cost (USD)	6,787,470 (5.15%)
total installed cost (USD)	1,052,900 (0.80%)
total equipment cost (USD)	162,000 (0.12%)
total utilities cost (USD/y)	73,700 (0.06%)
profit (USD/y)	83,447,242 (63.35%)
desired rate of return (%/y)	20
payout period (y)	3.23

[a]The number in the parentheses is the percentage based on the product's selling price.

4. CONCLUSIONS

A highly stable BTO in the form of a tetra-ester was successfully prepared via transesterification of POME and Di-TMP in the presence of $NaOCH_3$ as the basic catalyst. The optimum reaction condition was identified as a 5.0/1.0 POME/Di-TMP molar ratio in the presence of 8 mol % $NaOCH_3$ (based on the Di-TMP content) under 3.5 mbar with a stirring rate of 300 rpm

https://doi.org/10.1021/acsomega.4c05987
ACS Omega 2024, 9, 42396−42409

at 160 °C for 2 h. This process resulted in a 90.3% POME conversion level and 96.6% POME-Di-TMPTTE selectivity. The properties of the prepared BTO containing various POME-Di-TMPTTE proportions (70−97%) were compared to those of the IEC 62770 specification and Envirotemp FR3, a commercial BTO. The results showed that the BTO with a higher POME-Di-TMPTTE proportion exhibited superior oxidation stability, dielectric breakdown voltage, and flash point compared to Envirotemp FR3. However, the prepared BTO had a high kinematic viscosity at 40 °C (94.9−96.7 mm^2/s) and a high pour point (10−17 °C) that both exceeded the limitation of the IEC 62770 specification. This was attributed to the long-chain saturated fatty acids with a high molecular weight in the POME-Di-TMPTTE structure. The TEA revealed that the transesterification of POME and Di-TMP to produce BTO with a high proportion of POME-Di-TMPTTE showed promising potential for commercialization due to its competitive cost and profit margins relative to the selling price of Envirotemp FR3.

■ ASSOCIATED CONTENT

Supporting Information

The Supporting Information is available free of charge at https://pubs.acs.org/doi/10.1021/acsomega.4c05987.

Condition applied for GC-FID analysis and preparation of standard MeO-Di-TMPE via transesterification of MeO and Di-TMP (PDF)

■ AUTHOR INFORMATION

Corresponding Authors

Boonyawan Yoosuk − *Clean Fuel Technology and Advanced Chemistry Research Team, National Energy Technology Center, National Science and Technology Development Agency, Pathum Thani 12120, Thailand;* orcid.org/0000-0003-2107-1150; Email: boonyawan.yoo@entec.or.th

Napida Hinchiranan − *Department of Chemical Technology, Faculty of Science, Chulalongkorn University, Bangkok 10330, Thailand; Center of Excellence in Catalysis for Bioenergy and Renewable Chemicals (CBRC), Chulalongkorn University, Bangkok 10330, Thailand;* orcid.org/0000-0003-2384-257X; Phone: (66) 2218-7516; Email: napida.h@chula.ac.th

Authors

Ratchayol Sornvoralop − *Department of Chemical Technology, Faculty of Science, Chulalongkorn University, Bangkok 10330, Thailand*

Benjapon Chalermsinsuwan − *Department of Chemical Technology, Faculty of Science, Chulalongkorn University, Bangkok 10330, Thailand;* orcid.org/0000-0002-3372-9960

Nathapol Pintuyothin − *Department of Chemical Technology, Faculty of Science, Chulalongkorn University, Bangkok 10330, Thailand*

Complete contact information is available at: https://pubs.acs.org/10.1021/acsomega.4c05987

Notes

The authors declare no competing financial interest.

■ ACKNOWLEDGMENTS

The authors acknowledge The 100thAnniversary Chulalongkorn University Fund for Doctoral Scholarship; The 90th Anniversary Chulalongkorn University Fund (Ratchadaphiseksomphot Endowment Fund); the Agricultural Research Development Agency (ARDA; CPR6705030510); and the National Energy Technology Center (ENTEC), National Science and Technology Development Agency (NSTDA), for providing laboratory facilities and financial support. The authors extend their gratitude to Supphathee Chaowamalee for his invaluable advice on utilizing Aspen Plus V9 software for TEA.

■ ABBREVIATIONS

ATR−FTIR	attenuated total reflectance−Fourier-transform infrared spectroscopy
BTO	biotransformer oil
Di-TMP	ditrimethylolpropane
Di-TMPTTE	ditrimethylolpropane tetra-ester
FFA	free fatty acids
FP	flash point
GC-FID	gas chromatography with a flame ionization detector
MeO	methyl oleate
MeO-Di-TMPE	Di-TMP esters prepared from transesterification of MeO and Di-TMP
MO	mineral oil
MSTFA	*N*-methyl-*N*-trimethylsilyl trifluoroacetamide
NMR	nuclear magnetic resonance
O/A	mole ratio of PO derivative/neo-polyol
PE	pentaerythritol
PETTE	pentaerythritol tetra-ester
PO	palm oil
POEs	polyol esters
POME	palm oil methyl ester
POME-Di-TMPDE	diester derived from transesterification of POME and Di-TMP
POME-Di-TMPME	monoester derived from transesterification of POME and Di-TMP
POME-Di-TMPTE	triester derived from transesterification of POME and Di-TMP
POME-Di-TMPTTE	tetra-ester derived from transesterification of POME and Di-TMP
PP	pour point
RBDPO	refined-bleached-deodorized palm oil
SR	stirring rate
TEA	techno-economic analysis
TGA	thermogravimetric analysis
TMP	trimethylolpropane
TMPTE	trimethylolpropane triester
TO	transformer oil

■ REFERENCES

(1) Global electricity consumption 1980−2021. https://www.statista.com/statistics/280704/world-power-consumption/ (accessed 2024-05-05).

(2) Outlook for electricity. https://www.iea.org/reports/world-energy-outlook-2022/outlook-for-electricity (accessed 2024-05-05).

(3) Furqaranda, R.; Bintoro, A.; Asri, A.; Al-Ani, W. K. A.; Shrestha, A. Analysis oil condition of transformer PT-8801-A by using the method TDCG, Rogers ratio, key gas, and Duval triangle: a case study at PT. Perta Arun Gas. *JREECE* **2022**, *2* (2), 47.

(4) Transformer market size - by core (closed, shell, berry), by product (distribution transformer, power transformer, instrument transformer), by winding (two winding, auto-transformer), cooling, insulation, rating, mounting, application & forecast, 2023 − 2032. https://www.gminsights.com/industry-analysis/transformer-market (accessed 2024-05-05).
(5) Transformer oil market outlook 2022−2032. https://www.persistencemarketresearch.com/market-research/transformer-oil-market.asp (accessed 2024-05-05).
(6) Shen, Z.; Wang, F.; Wang, Z.; Li, J. A critical review of plant-based insulating fluids for transformer: 30-year development. *Renewable Sustainable Energy Rev.* **2021**, *141*, 110783.
(7) Aluyor, E. O.; Ori-Jesu, M. Biodegradation of mineral oils − a review. *Afr. J. Biotechnol.* **2009**, *8* (6), 915−920.
(8) Raof, N. A.; Yunus, R.; Rashid, U.; Azis, N.; Yaakub, Z. Palm-Based neopentyl glycol diester: a potential green insulating oil. *Protein Pept. Lett.* **2018**, *25* (2), 171−179.
(9) Rozga, P.; Beroual, A.; Przybylek, P.; Jaroszewski, M.; Strzelecki, K. A review on synthetic ester liquids for transformer applications. *Energies* **2020**, *13* (23), 6429.
(10) Stuchala, F.; Rozga, P.; Malaczek, M.; Staniewski, J. Comparative analysis of selected insulating liquids including bio-based hydrocarbon and GTL in terms of breakdown and acceleration voltage at negative lightning impulse. *IEEE Trans. Dielectr. Electr. Insul.* **2024**, *1*, 1.
(11) Badawi, M.; Ibrahim, S. A.; Mansour, D.-E. A.; Ward, S. A.; El-Faraskoury, A.; Ghali, M.; Mahmoud, K.; Lehtonen, M.; Darwish, M. M. F. On Highlighting the Merits of Gas-To-Liquid Transformer Oil under Accelerated Thermal Aging and Faults: Electrical and Physio-chemical Properties. *IEEE Access* **2024**, *12*, 93372−93388.
(12) Sequiño, A. C.; Abocejo, F. T. The palm oil industry in the Philippines and Thailand: Challenges and opportunities. In *34th International Business Information Management Association (IBIMA) Conference Proceedings: Madrid*, 2019, pp 13267−13279.
(13) Worldwide production major vegetable oils 2012−2023. https://www.statista.com/statistics/263933/production-of-vegetable-oils-worldwide-since-2000/ (accessed 2024-05-05).
(14) Irwan, S.; Yaakob, Z.; Kumar, M. N. S.; Primandari, S. R. P.; Kamarudin, S. K. Biodiesel progress in Malaysia. *Energy Sources, Part A* **2012**, *34* (23), 2139−2146.
(15) Karthik, M.; Narmadhai, N. A survey on natural esters based insulating fluid medium for transformer applications. *Mater. Today: Proc.* **2021**, *45*, 2022−2028.
(16) Raof, N. A.; Yunus, R.; Rashid, U.; Azis, N.; Yaakub, Z. Effect of molecular structure on oxidative degradation of ester based transformer oil. *Tribol. Int.* **2019**, *140*, 105852.
(17) Raof, N. A.; Hamid, H. A.; Mohamad Aziz, N. A.; Yunus, R. Prospects of plant-based trimethylolpropane esters in the biolubricant formulation for Various applications: A review. *Front. Mech. Eng.* **2022**, *8*, 833438.
(18) Salih, N.; Salimon, J.; Yousif, E.; Abdullah, B. M. Biolubricant basestocks from chemically modified plant oils: ricinoleic acid based-tetraesters. *Chem. Cent. J.* **2013**, *7* (1), 128.
(19) Baskar, G.; Kalavathy, G.; Aiswarya, R.; Selvakumari, I. A. Advances in bio-oil extraction from nonedible oil seeds and algal biomass. In *Advances in Eco-Fuels for a Sustainable Environment*, 2019; pp 187−210..
(20) Aziz, N. A. M.; Hamid, H. A.; Yunus, R.; Abbas, Z.; Omar, R.; Rashid, U.; Syam, A. M. Kinetics and thermodynamics of synthesis of palm oil-based trimethylolpropane triester using microwave irradiation. *J. Saudi Chem. Soc.* **2020**, *24* (8), 552−566.
(21) Aziz, N. A. M.; Yunus, R.; Rashid, U.; Syam, A. M. Application of response surface methodology (RSM) for optimizing the palm-based pentaerythritol ester synthesis. *Ind. Crop. Prod.* **2014**, *62*, 305−312.
(22) Idrus, N. F.; Yunus, R.; Zainal Abidin, Z.; Rashid, U.; Abd Rahman, N. High oleic pentaerythritol tetraester formation via transesterification: Effect of reaction conditions. *Indones. J. Chem.* **2020**, *20* (4), 887.
(23) Bahadi, M.; Salimon, J.; Derawi, D. Synthesis of di-trimethylolpropane tetraester-based biolubricant from *Elaeis guineensis* kernel oil via homogeneous acid-catalyzed transesterification. *Renewable Energy* **2021**, *171*, 981−993.
(24) Cecilia, J. A.; Ballesteros Plata, D.; Alves Saboya, R. M.; Tavares de Luna, F. M.; Cavalcante, C. L.; Rodríguez-Castellón, E. An overview of the biolubricant production process: challenges and future perspectives. *Processes* **2020**, *8* (3), 257.
(25) Vicente, G.; MartíNez, M.; Aracil, J. Integrated biodiesel production: a comparison of different homogeneous catalysts systems. *Bioresour. Technol.* **2004**, *92* (3), 297.
(26) Cruze, A. P.; Lokesh, K. S. Ageing Characteristics of alkali neutralized neem oil for liquid insulation. *International Conference on High Voltage Engineering and Technology (ICHVET)*; IEEE: Hyderabad, 2019; pp 1−5.
(27) Devitasari, R. D.; Fathurrahman, N. A.; Katili, M.; Wibowo, C. S.; Bethari, S. A.; Anggarani, R.; Aisyah, L.; Maymuchar, N. Determination of oxidation stability of palm-oil biodiesel and Biodiesel-Diesel blends by Rancimat and RSSOT methods. *IOP Conf. Ser. Earth Environ. Sci.* **2022**, *1034* (1), 012040.
(28) Kurniawan, Y. S.; Ramanda, Y.; Thomas, K.; Hendra, H.; Wahyuningsih, T. D. Synthesis of 1,4-dioxaspiro[4.4] and 1,4-dioxaspiro[4.5] novel compounds from oleic acid as potential biolubricant. *Indones. J. Chem.* **2017**, *17* (2), 301−308.
(29) Jumaah, M. A.; Khaleel, F. L.; Salih, N.; Salimon, J. Synthesis of tri, tetra, and hexa-palmitate polyol esters from Malaysian saturated palm fatty acid distillate for biolubricant production. *Biomass Convers. Bior.* **2024**, *14* (2), 1919−1937.
(30) Chira, N. A.; Nicolescu, A.; Stan, R.; Rosca, S. Fatty acid composition of vegetable oils determined from ^{13}C-NMR spectra. *Rev. Chim.* **2016**, *67* (7), 1257−1263.
(31) Fukuda, H.; Kondo, A.; Noda, H. Biodiesel fuel production by transesterification of oils. *J. Biosci. Bioeng.* **2001**, *92* (5), 405−416.
(32) Gunam Resul, M. F. M.; Mohd Ghazi, T. I.; Idris, A. Kinetic study of jatropha biolubricant from transesterification of *Jatropha curcas* oil with trimethylolpropane: Effects of temperature. *Ind. Crop. Prod.* **2012**, *38*, 87.
(33) Flowers, P.; Theopold, K.; Langley, R. Fundamental equilibrium concepts. In *Chemistry*; OpenStax College, 2015; pp 729−776.
(34) Yunus, R.; Fakhru'l-Razi, A.; Ooi, T. L.; Iyuke, S. E.; Idris, A. Development of optimum synthesis method for transesterification of palm oil methyl esters and trimethylolpropane to environmentally acceptable palm oil-based lubricant. *J. Oil Palm Res.* **2003**, *15*, 35−41.
(35) Koh, M. Y.; Mohd Ghazi, T. I.; Idris, A. Synthesis of palm based biolubricant in an oscillatory flow reactor (OFR). *Ind. Crop. Prod.* **2014**, *52*, 567−574.
(36) Kamil, R. N. M.; Yusup, S.; Rashid, U. Optimization of polyol ester production by transesterification of Jatropha-based methyl ester with trimethylolpropane using Taguchi design of experiment. *Fuel* **2011**, *90* (6), 2343−2345.
(37) Sharma, Y. C.; Singh, B.; Korstad, J. High yield and conversion of biodiesel from a nonedible feedstock (Pongamia pinnata). *J. Agric. Food Chem.* **2010**, *58* (1), 242−247.
(38) Jasińska, M. Test reactions to study efficiency of mixing. *Chem. Process Eng.* **2015**, *36* (2), 171.
(39) Boyde, S. Organic Esters. In *Encyclopedia of Tribology*; Wang, Q. J., Chung, Y. W., Eds.; Springer, 2013; pp 2493−2500.
(40) Williams, T. J.; Cherepakhin, V. Direct oxidation of primary alcohols to carboxylic acids. *Synthesis* **2021**, *53* (06), 1023−1034.
(41) ENVIROTEMP FR3 Fluid; CAS RN: 8001−22−7; Cargill; Retrieved from VanTran Transformers. December 14, 2017. https://vantran.com/wp-content/uploads/2020/12/Envirotemp-FR3-SDS.pdf (accessed 2024-05-08).
(42) Fox, N. J.; Stachowiak, G. W. Vegetable oil-based lubricants—A review of oxidation. *Tribol. Int.* **2007**, *40* (7), 1035−1046.
(43) Brown, T. L.; LeMay, H. E.; Bursten, B. E.; Murphy, C. J.; Woodward, P. M.; Stoltzfus, M. W.; Lufaso, M. W. *Chemistry: The Central Science*, 14th ed.; Pearson, 2017.
(44) Prince, R. J. Base oils from petroleum. In *Chemistry and Technology of Lubricants*; Mortier, R. M., Fox, M. F., Orszulik, S. T., Eds.; Springer, 2010; pp 7−12.

https://doi.org/10.1021/acsomega.4c05987
ACS Omega 2024, 9, 42396−42409

(45) Brown, M.; Fotheringham, J. D.; Hoyes, T. J.; Mortier, R. M.; Orszulik, S. T.; Randles, S. J.; Stroud, P. M. Synthetic base fluids. In *Chemistry and Technology of Lubricants*; Mortier, R. M., Fox, M. F., Orszulik, S. T., Eds.; Springer, 2010; pp 54−58.
(46) Karthik, S.; Rahman, H.; Balakumar, K.; Duganath, N.; Chandrasekar, R.; Hariprasad, R. Pharmaceutical nanotechnology: Brief perspective on lipid drug delivery and its current scenario. In *Biomedical Applications of Nanoparticles*; Grumezescu, A. M., Ed.; William Andrew, 2019; pp 91−115.
(47) Raof, N. A.; Yunus, R.; Rashid, U.; Azis, N.; Yaakub, Z. Effects of palm-based trimethylolpropane ester/mineral oil blending on dielectric properties and oxidative stability of transformer insulating liquid. *IEEE Trans. Dielectr. Electr. Insul.* **2019**, *26* (6), 1771−1778.
(48) Islam, M. M.; Hassan, M. H.; Kalam, M. A.; Zulkifli, N. W. B. M.; Habibullah, M.; Hossain, M. M. Improvement of cold flow properties of *Cocos nucifera* and *Calophyllum inophyllum* biodiesel blends using polymethyl acrylate additive. *J. Clean. Prod.* **2016**, *137*, 322−329.
(49) Sumathi, S.; Rajesh, R. Improvement on the characteristics of transformer oil using nanofluids. *Curr. Sci.* **2020**, *118* (1), 29−33.
(50) Biodiesel prices (SME & FAME). https://www.neste.com/investors/market-data/biodiesel-prices (accessed 2024-05-10).
(51) Di-TMP 98% Di-Trimethylolpropane of white flakes. https://rawchem2021.en.made-in-china.com/product/vFufWBaKkXkc/China-Di-TMP-98-Di-Trimethylolpropane-of-White-Flakes.html (accessed 2024-05-10).
(52) CAS 124−41−4 good factory price sodium methylate solid sodium methoxide. https://www.alibaba.com/product-detail/CAS-124-41-4-good-factory_1600076586177.html?spm=a2700.7724857.0.0.407b6f15fCEYMl (accessed 2024-05-10).
(53) Factory outlet methanol 99.9% purity CAS No. 67−56−1 with best price. https://www.alibaba.com/product-detail/Methanol-Methanol-Factory-Outlet-Methanol%2099_1600768748411.html?spm=a2700.gallery%20offerlist.%20p_offer.d_price.71c76672B24eix&s=p (accessed 2024-05-10).
(54) Envirotemp FR3 Fluid 55USG Drum. https://www.silmid.com/us/lubricants/metal-working-lubricants/envirotemp-fr3-fluid-55usg-drum/ (accessed 2024-05-10).
(55) Electricity prices for enterprises worldwide in June 2023, by select country. https://www.statista.com/statistics/1369634/business-electricity-price-worldwide-in-selected-countries/?gad_source=1&gclid=Cj0KCQiAw6yuBhDrARIsACf94RU2clTOJSTlL3G-XsCPOp5EeW6J6FtOdNCcyPk_0fz98AnWf8TSBHAaAr_aEALw_wcB (accessed 2024-05-10).

https://doi.org/10.1021/acsomega.4c05987
ACS Omega 2024, 9, 42396−42409